GEOPHYSICAL RESEARCH LETTERS, VOL. 25, NO.14, PAGES 2613-2616, JULY 15, 1998

A pair of forward and reverse slow-mode shocks detected by Ulysses at ~ 5 AU

C. M. Ho[1], B. T. Tsurutani[1], N. Lin[2], L. J. Lanzerotti[3], E.J. Smith[1], B.E.Goldstein[1], B. Buti[1], G. S. Lakhina[1], and X. Y. Zhou[1]

Abstract. We report the first finding of a pair of forward and reverse slow-mode shocks in the distant heliosphere using plasma and magnetic field data from the Ulysses spacecraft located at 5.3 AU and 9° S heliolatitude. The slow-mode shocks are found to occur in a compressed magnetic field (low plasma) region within a co-rotating interaction region (CIR). We find Mach numbers to be 0.3-0.5 with respect to forward/reverse slow shocks. Across each shock, the solar wind velocities jump by at least 40 km/s. The increases in plasma density and ion temperature accompany a decrease in the magnetic field. The shocks are also found to have velocities of 60 km/s and 115 km/s and thicknesses between 7.5 - 12.6 x 10^4 km (much larger than the ion inertial length, ~ 10^3 km). Low frequency plasma waves are detected by the Ulysses URAP instrument at the slow-mode shock transition regions. However, the waves are not of sufficient amplitude to provide enough anomalous resistivity through wave-particle interactions for shock dissipation. Low energy (~30 - 90 keV) electron enhancements directed along the local magnetic field are also found associated with the slow shocks, indicating the ability of the shocks to accelerate interplanetary particles. This finding imply that more slow shocks might be found in the CIR magnetic compressed regions (where plasma is squeezed out) at large heliospheric distances.

Introduction

Interplanetary slow-mode shocks are fundamental micro-structures of the solar wind, which are of interest from the points of view of space plasma theory and heliospheric dynamics. Slow-mode shocks may play an important role in interplanetary space in magnetic reconnection and, thus, the heating of the solar wind plasma [Petschek, 1964]. Slow shocks can result from the steepening of MHD slow-mode waves. It is most probable that slow-mode shocks are generated in interplanetary regions [Barnes, 1966; Richter, 1991] where collisionless damping of slow-mode waves is small and the linear damping time exceeds the steepening time (i.e., plasma β $(8\pi k_B(n_pT_p+n_eT_e)/B^2) < 1$ and T_p / T_e <1). However, even though in the last several decades a significant amount of solar wind data have been accumulated, only a limited number of interplanetary slow-mode shocks (at or within 1 AU) have been reported/identified [Chao and Olbert, 1970; Burlaga and Chao, 1971; Richter, 1991].

Magnetohydrodynamic (MHD) theory [Kennel et al., 1985] shows that both fast and slow-mode shocks can propagate either away from (forward shocks) or towards (reverse shocks) the sun with respect to the solar wind frame. At large heliospheric distances, when a corotating high speed solar wind overtakes a low speed solar wind, a pair of forward and reverse fast shocks are usually formed [Smith and Wolfe, 1976]. Similar to the fast mode shocks, a pair of forward and reverse slow-mode shocks are expected to exist. Within MHD there exists the possibility that slow shocks can be generated behind fast shocks with non-zero normal magnetic field components (the so-called Riemann problem) [Rosenau and Suess, 1977]. For slow-mode shock, the plasma density, temperature and bulk velocity increase, and the magnetic field decreases (unlike the fast shock case where filed increases) as schematically illustrated in Figure 1. Thus there is a higher plasma beta (β) region between the shocks than in the region outside them. We report here the discovery of a pair of forward and reverse slow-mode shocks through an extensive search of Ulysses interplanetary data.

Data and Method

The magnetic field (1 min. time resolution) and plasma (4 min. maximum sample rate) data measured on Ulysses are used for the slow-mode shock search and identification. The coordinate system is a RTN system, where $\bar{R}$ is the radial direction from the Sun, $\bar{T} = \bar{\Omega} \times \bar{R} / |\bar{\Omega} \times \bar{R}|$ ($\bar{\Omega}$ is the solar rotation axis), and $\bar{N}$ completes the right-hand system. Plasma wave data and energetic particle data measured on Ulysses are also used to identify their associated signatures with the slow shocks. Description of all instruments can be found in the Supplementary Serials (Volume 92) of *Astronomy and Astrophysics* [1992].

The method used to identify the slow shocks is similar to that developed in a study of slow shocks in the geomagnetic tail [Ho et al., 1996]. We first determine if both conditions of β < 1 (i.e., magnetic pressure less than plasma thermal pressure) and $T_p < T_e$ are satisfied in the interval. Then we next examine the jump conditions in the magnetic field, plasma temperature, density, and solar wind velocity for the shock candidate events. We use the coplanarity theorem to calculate the shock normal in order to find the magnetic field normal component (magnetic flux) and velocity components (mass flux). The magnetic field geometry and the total pressure change across the shock are also checked using Rankine-Hugoniot relations. Finally, the slow shock is verified by the criteria: $V_{sl} < V_n^* \leq V_{An}$, where V_{sl} is the slow mode speed. The

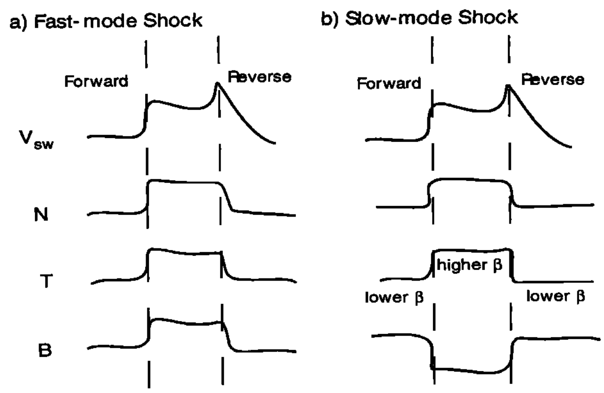

Figure 1. A cartoon showing differences in IMF and plasma changes across a pair of forward and reverse fast-mode shocks (a) from a pair of forward and reverse slow-mode shocks (b).

[1]Jet Propulsion Laboratory, California Institute of Technology, Pasadena, CA 91109

[2]School of Physics and Astronomy, University of Minnesota, Minneapolis, MN 55455

[3]Bell Laboratories, Lucent Technologies, Murray Hill, NJ 07974

Paper number 98GL02014.
0094-8534/98/98GL-02014$05.00

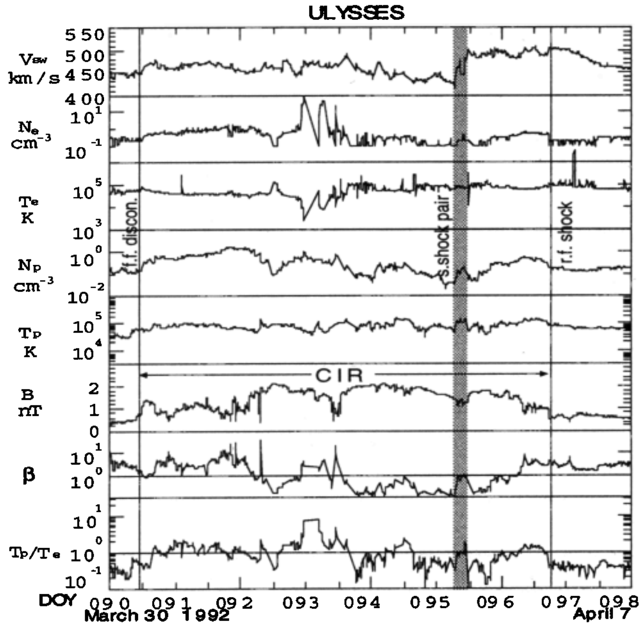

Figure 2. Slow shock location relative to a compressed magnetic field region inside a CIR. The pair of slow shocks (which interval is shaded) are in the rear portion of the CIR as marked.

Alfvén velocity is $V_A = B/(4\pi N m_p)^{1/2}$ and $V_n^* = (\vec{V}-\vec{V}_s)\cdot\vec{n}$, is the solar wind velocity $\vec{V}$ relative to the shock velocity, $\vec{V}_s$, along the shock normal, $\vec{n}$, the latter which is obtained through coplanarity analyses. Defining the Alfvén velocity along the normal $V_{An} = V_A \cos\theta_{Bn}$, the Alfvén Mach number (which alway has ≤1) is $M_A = V_n^* / V_{An}$, where θ_{Bn} is the angle between the magnetic field and shock normal.

Results

Beyond 1 AU, in the ecliptic plane, the solar wind expands and stream-stream interactions become more pronounced. Large numbers of co-rotation interacting region (CIR) structures, fast forward, and fast reverse shocks have been detected. In these regions, high speed solar wind streams interact with low-speed streams, leading to a compression and pile-up of the plasma and magnetic field in front of the leading edges of the fast streams. Because of this interaction, hydromagnetic stresses propagate into both the slow and fast streams as large amplitude waves which ultimately steepen into a forward shock at the leading edge of a CIR and a reverse shock at the trailing edge. This effect becomes more significant with increasing heliocentric distances from the sun. Slow-mode shocks might be expected to originate at boundaries between lower and high beta regions. After surveying first two years of Ulysses data, we have found 11 slow-mode shock candidates in the low latitude solar wind. They all are present in the CIR magnetic compression regions. Only 4 of them are confirmed as slow-mode shocks through our slow shock identification procedure.

The pair of slow-mode shocks analyzed here is found in a compressed magnetic field region within a CIR. This region is bounded by both a fast forward shock-like discontinuity (f.f. discon.) and a reverse fast shock (r.f. shock) as marked in Figure 2. This CIR was encountered after Jupiter flyby when Ulysses was enroute to the southern heliosphere (5.3 AU and 8.8°S heliographic latitude). Within the compressed magnetic field region, the magnetic field increases by about factor 4 relative to the outside uncompressed region. In the same time, changes in the plasma density and temperature are not obvious. It is possible that the plasma inside is squeezed out along the CIR magnetic fields at the flanks. Thus, the compressed region has a low value of β (< 1.0) relative to the non-compression regions.

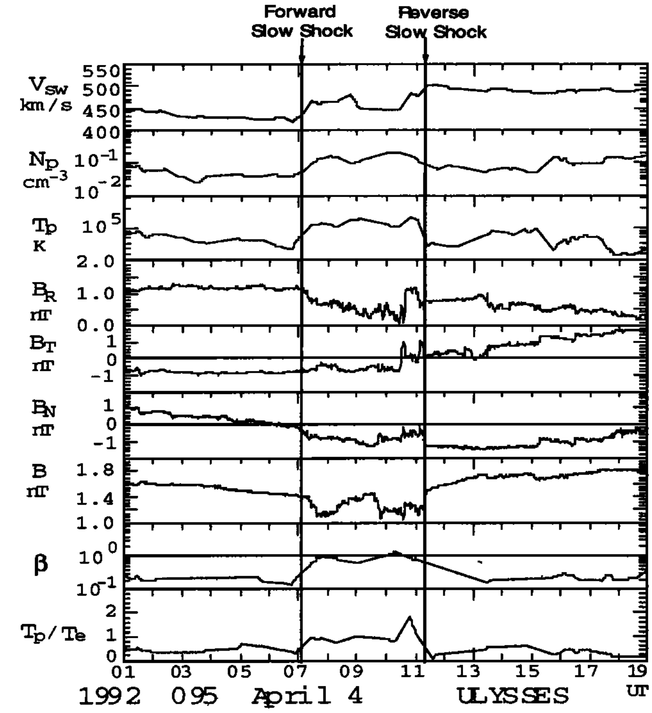

Figure 3. A pair of slow-mode shocks identified. From top to bottom are, solar wind speed, ion density and temperature, three magnetic field components and magnitude (with 1 min. resolution), plasma β and ratio of *Tp* to *Te*.

This pair of slow shocks actually occurred in the latter portion of the CIR, about one day before the reverse fast shock. We have expanded this period of data in Figure 3. The plasma properties are seen to be similar to those predicted by theory (Figure 1). The remarkable feature is the significant velocity jumps associated with both discontinuities (marked by vertical lines). At the first discontinuity (0710 UT on April 4, 1992) the velocity V_{Sw} increases from 425 km/s to 463 km/s. Proton density (n_p) increases from 0.6 to 1.2 cm^{-3} while the proton temperature T_p jumps from 0.4 to 0.5×10^5K. In contrast to these increases, the magnetic field decreases from 1.4 to 1.1 nT. After the decrease, the magnetic field has a gradual increase but then returns to the previous low level. The second interplanetary discontinuity occurred at 1105 UT. The

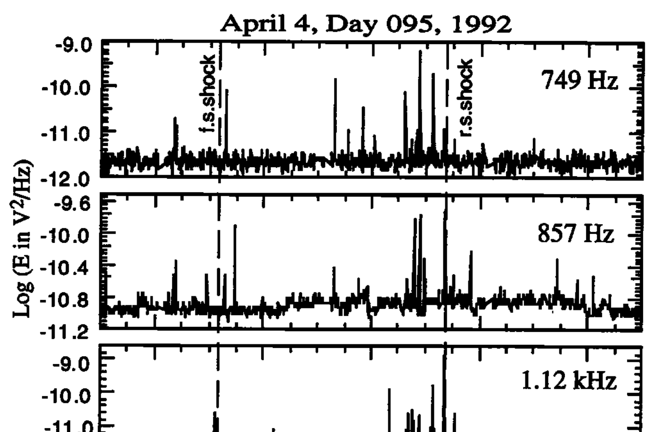

Figure 4. Plasma wave bursts associated with shocks. The waves appearing in three electric field narrowband channels are probably ion acoustic waves. Dotted lines show the total magnetic field.

Table 1. Time Interval Selected and Average Magnetic Field Values

	Forward Shock		Reverse Shock	
	Upstream	Downstream	Downstream	Upstream
Time Interval	06:15 -06:35UT	07:45 -08:10UT	10:05-10:20UT	13:15-13:50UT
B in **RTN** (nT)	1.13, -0.89, -0.04	0.67, -0.41, -0.82	0.35, -0.69, -0.88	0.70, 0.50, -1.44
B in **IJK** (nT)	0.90, 0.01, 1.12	-0.12, 0.01, 1.12	-0.16, 0.01, 1.16	1.22, 0.01, 1.16

magnetic field increases from 1.2 to 1.7 nT and V_{sw} increases from 447 km/s to 500 km/s. n_p decreases from 0.2 to 0.07cm^{-3} while T_p decreases from 1.5 to 0.6x10^{5}K. Within the downstream region (between the two shocks) there are higher plasma β (~1) and Tp/Te ratio (> 0.6). We have also noted that there is a delay for forward shock in the total magnetic field decrease relative to the increases in the solar velocity and plasma. However, the changes in both B_R and B_N components occur almost simultaneously relative to plasma changes. The changes in both components may cancel each other so that the B magnitude appears to change later.

We have first used the coplanarity theorem to determine the shock normal. Both upstream and downstream intervals and magnetic feild components are listed in Table 1. Then using our slow shock criteria and 3-D solar wind velocity and plasma data, both discontinuities are confirmed as slow-mode shocks. The first one is a forward shock, while the second one is a reverse shock. All shock parameters are showed in Table 2. The errors are about 5% in both shock normal and velocity determination (based on standard deviation estimate), assuming that these regions are genuinely representative of the upstream and downstream conditions at the shocks. Both slow shock normals are mainly in the N (or latitudinal) direction. This result is consistent with fast shock's orientation. In a recent study, Burton et al. [1996] studied ~80 fast shocks detected by Ulysses out of ecliptic plane. They found that the shocks propagate both equatorward and poleward. This is also consistent with the model of Pizzo [1991]. The shock front often is formed due to the interaction between the low latitude slow wind and high latitude fast wind.

For both slow shocks, their downstream θ_{Bn} is less than the upstream angle because of the weak downstream magnetic field. This is consistent with a slow shock's geometry. Their Alfvén Much numbers are between 0.31 and 0.50. The shocks are quite weak because the plasma velocity is very close to the V_{sl}. We also find that across the shocks the total pressure (magnetic plus thermal pressure) increases slightly. This is the main difference from a tangential discontinuity.

Table 2. Parameters for Pair of Slow-mode Shocks

Shock Parameters	Forward Shock 0710UT	Reverse shock 1105UT
n in RTN	-0.30, 0.32, 0.90	0.34, -0.48, -0.81
B_1, nT	1.44	1.71
B_2, nT	1.14	1.18
B_n, nT	1.12	1.16
θ_{Bn1}	39°	47°
θ_{Bn2}	10°	10°
V_1, km/s	424	499
V_2, km/s	465	447
N_{p1}, cm^{-3}	0.04	0.07
N_{p2}, cm^{-3}	0.10	0.20
T_{p1}, x10^{5}K	0.50	0.59
T_{p2}, x10^{5}K	1.10	1.45
V_s, km/s	60	115
V_{An}, km/s	92	87
V_n^*, km/s	29	44
V_{sl}, km/s	26	20
M_A	0.31	0.50
ΔP_{tot}, dyn/cm^2	0.05x10^{-10}	0.01x10^{-10}

We have calculated the slow-mode shock speed using mass conservation and the electric field conservation in the shock frame [Smith and Burton, 1988], respectively. Both methods yield nearly the same value for V_s. For the forward shock, the shock speed is about 60 km/s, while the reverse shock has a speed about 115 km/s. The speeds are similar to those for fast shocks. Burton et al. [1996] showed that fast shocks measured in Ulysses data between 4.0 and 5.0 AU have speeds ranging from 80 km/s to 180 km/s.

Using the shock speed, the shock thickness (λ_s) may be estimated by measuring the magnetic field jump interval. For the forward shock, the jump interval is about 25 min (0710 - 0735 UT), while for the reverse shock, it is ~20 min (1100 - 1120 UT). After removing the spacecraft motion (Vsc = ~10 km/s in N direction), we find shock thicknesses of 7.5x10^4 km and 12.6x10^4 km, respectively. This is equivalent to 65 and 144 ion inertial lengths (c/ω_{pi} ~ 10^3 km). This thickness is much larger than those of the slow shocks detected in the distant geomagnetic tail [Ho et al., 1995]. A theoretical study [Coroniti, 1971] suggests that slow shocks should have thicknesses of ~ 3-6 c/ω_{pi}. One scenario explaining these large thickness is that the pair of shocks could have propagated some distance upstream after they were generated. The slow shocks become thicker because of solar wind velocity dispersion. Slow shocks will eventually disappear/dissipate as they propagate outward. They will be further weakened until their Mach number becomes close to unity, and then become a tangential discontinuity [Rosenau and Suess, 1977].

The slow shock dissipation mechanism is not well understood. It has been found that broadband plasma waves with frequencies ranging from ULF to VLF are detected in and near the shock layer in the distant geotail [Scarf et al., 1984]. The anomalous resistivity provided by the waves has been used to explain shock dissipation [Coroniti, 1971]. If such plasma waves are detected in interplanetary space associated with slow shocks, we can calculate the anomalous resistivity due to the waves and compare this with theoretical models. We have found that some wave bursts are detected by the Ulysses plasma wave instrument during the shock interval. Figure 4 shows the wave bursts measured from E_x antenna in three narrowband frequency channels (749, 857, and 1120 Hz) that occurred in the shock transition regions. These waves are similar to those observed at directional discontinuities and in magnetic holes

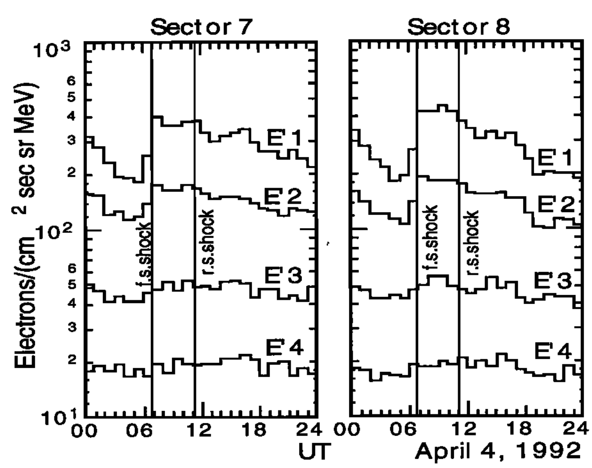

Figure 5. HI-SCALE measurements for energetic electrons during the slow shocks from low to high energy channels. In the directional sectors 7 (left) and 8 (right), there are significant electron enhancements in two low energy channels (E'_1 and E'_2) around the shocks.

[Lin et al., 1995] and near interplanetary shocks reported previously [Hess et al., 1998]. Considering the electron plasma frequency f_{pe} ~3 kHz, proton plasma frequency f_{pi} ~ 67 Hz, electron gyrofrequency f_{ce} ~ 44 Hz, proton gyrofrequency f_{ci} ~ 0.025 Hz, and the lower hybrid frequency f_{lh} ~ 1.1 Hz, these wave bursts are likely to be ion acoustic waves which have been Doppler-shifted to the observed frequencies.

If indeed these ion acoustic waves provide anomalous resistivity to cause the shock damping, the magnetic Reynolds length (r_m) should have the same order as the shock thickness λ_s [Coroniti, 1971]. However, using all measured values, the calculation shows that r_m (=1/7500 c/ω_{pi}) is far less than the λ_s (~50 c/ω_{pi}). Thus, this inconsistency suggests that the slow shock dissipation was not caused by an ion acoustic anomalous resistivity. The shock dissipation should be caused by some other mechanism(s). However, the upstream ion acoustic waves may suggest the existence of an ion foreshock in front of the forward slow shock.

We have examined hourly average measurements of energetic particles from the HI-SCALE instrument [Lanzerotti, et al., 1992] during the period of the slow shock pair. Strong electron enhancements are detected in the two lowest energy channels (30-50 keV, and 50-90 keV). The enhancements are mainly seen in the direction of sectors 7 and 8 in telescope LEFS60, beginning about 07 UT and ending at 13 UT, as shown in Figure 5. The enhancements are less obvious in the two highest energy channels (90-165 keV, and 165-300 keV). LEFS60 has a 60° central view angle relative to the spin axis of the spacecraft. Around the spin axis, which is always pointed to the Earth, there are 8 directional sectors. The data are sampled in each sector every 12 s rotation period. Analysis shows that during this period, the magnetic fields are in the direction of sectors 7 and 8. Thus, these particles are propagating primarily along the background magnetic field. Since there are strong anisotropies in the pitch angle for these electrons (approximately 4 to 1 front to back anisotropy at the lowest energies), they are definitely accelerated by the slow shocks. Because both slow shocks are near quasi-parallel (θ_{Bn} < 50°), magnetostatic reflection off the shock may be a significant acceleration mechanism [Tsurutani and Lin, 1985]. An initial investigation shows that lower energy protons (50-73 keV) also show some enhancements around the slow shock. However, compared with the electrons, the enhancements in the energetic proton flux are smaller. A detailed analysis of the energetic electron acceleration by the slow shocks will be reported elsewhere.

Summary

This is the first slow shock pair (forward/reverse) discovered in interplanetary space. The shocks were embedded inside a CIR. In our study we have also detected four other (forward) slow shocks. All of the events were found within CIRs. We are surprised to find pockets of such low beta regions (~0.1) within CIRs. One possible explanation is that the plasma is squeezed out along the CIR magnetic fields at the flanks. These low beta regions allow formation of slow shocks because the Alfvén speed is greater than the sound speed there. If this mechanism is the correct one, then there might be many more slow shocks at large heliocentric distance, e.g., to be detected by the Cassini mission.

The slow shock normal we found in this study is mainly along the N (latitudinal) direction, consistent with fast mode shocks and the model predicted. The downstream magnetic field θ_{Bn} is less than the upstream θ_{Bn}. The total pressure increases slightly across the shock from upstream to downstream. These properties are consistent with predictions for slow shocks. For both the forward and reverse shocks, the shock speeds are found to be 60 km/s and 115 km/s, respectively, similar to fast-mode shocks found in Ulysses measurements. Based on the shock ramp durations and the speeds, the calculated shock thickness is 7.5 ~ 12.6x10^4 km, equivalent to 65 ~ 144 c/ω_{pi}. The thickness is much larger than those of slow shocks detected in the distant geotail and also larger than their inertial length as predicted by theory. This implies that the shocks have propagated some distance after their generation.

Low frequency wave bursts are found in the shock transition regions. These waves are probably ion acoustic waves. Calculations show that these waves cannot provide enough anomalous resistivity through wave-particle interactions for dissipation of the shock. We also find strong electron enhancements in two low energy channels (30-50 keV, and 50-90 keV) around the shocks. Electron peaks begin about one hour before the forward shock and end about one hour after the reverse shock. The electrons are dominantly propagating along the background magnetic field. Because the slow shocks are near quasi-perpendicular shocks (θ_{Bn} > 50°), magnetostatic reflection off the shock may be involved in the acceleration mechanism.

Acknowledgments: The research conducted at the Jet Propulsion Laboratory, California Institute of Technology was performed under contract to the National Aeronautics and Space Administration. The work done at the University of Minnesota was supported by NASA under contract NAS5-31219

References

Barnes, A., Collisionless damping of hydromagnetic waves, *Phys. Fluids, 9*, 1483, 1966.

Burton, M. E., et al., Ulysses out-of-ecliptic observations of interplanetary shocks, *Astron. Astrophys. 316*, 313, 1996.

Burlaga, L.F., and J.K.Chao, Reverse and forward slow shocks in the solar wind, *J. Geophys. Res., 76*, 7516, 1971.

Chao, J.K., and S. Olbert, Observation of slow shocks in interplanetary space, *J. Geophys. Res., 75*, 6394, 1970.

Coroniti, F.V., Laminar wave-train structure of collisionless magnetic slow shocks, *Nuclear Fusion, 11*, 261, 1971.

Hess, R.A., et al., Ion acoustic-like waves observed by Ulysses near interplanetary shock waves in the 3D heliosphere, *J. Geophys. Res., 103*, 6531, 1998.

Ho, C.M., et al., Properties of slow-mode shocks in the distant (> 200 R_e) geomagnetic tail, *J. Geophys. Res., 101*, 15277, 1996.

Kennel, C.F, et al., A quarter century of collisionless shock research, *AGU Geophys. Monogr. Ser., 34*, 1, edited by R.G.Stone and B.T.Tsurutani, Washington D.C., 1985.

Lanzerotti, L. J., et al., Heliospheric instrument for spectra, composition and anisotropy at low energies, *Astron. Astrophys. Suppl. Ser. 92*, 349, 1992.

Lin, N., et al., Observations of plasma waves in magnetic holes, *Geophys. Res. Letts., 22*, 3417, 1995.

Petschek, H.E., Magnetic field annihilation, *AAS-NASA symposium on the physics of solar flares, edted by W.N.Hess*, NASA SP-50, P425, 1964.

Pizzo, V. J., The evolution of corotating stream fronts near the ecliptic plane in the inner solar system 2: Three dimensional tilted-dipole fronts, *J. Geophys. Res., 96*, 5405, 1991.

Richter, A.K., Interplanetary slow shocks, Space and Solar Physics, *21*, 23, *Physics of the Inner Heliosphere II*, Editors, R. Schwenn, E. Marsch, Springer-Verlag Berlin Heidelberg, 1991.

Rosenau, P. and S.T. Suess, Slow shocks in interplanetary medium, *J. Geophys. Res., 82*, 3643, 1977

Scarf, F.L., et al., Plasma wave spectra near slow-mode shocks in distant magnetotail, *Geophys. Res. Lett., 11*, 1050, 1984.

Smith, E.J., and J.H.Wolfe, Observations of interaction region and corotating shocks between one and five AU: Pioneer 10 and 11, *Geophys. Res. Lett., 3*, 137, 1976.

Smith, E.J., and M.E. Burton, Shock analysis: Three useful new relations, *J. Geophys. Res., 93*, 2730, 1988.

Tsurutani, B.T., and R.P. Lin, Acceleration of > 47 keV ions and > 2keV electrons by interplanetary shocks at 1 AU, *J. Geophys. Res., 90*, 1, 1985.

C. M. Ho, B. T. Tsurutani, E.J. Smith, B.E.Goldstein, B. Buti, G. S. Lakhina, and X. Y. Zhou, Jet Propulsion Laboratory, California Institute of Technology, Pasadena, CA 91109 (email: cho@jplsp.jpl.nasa.gov)

N. Lin, School of Physics and Astronomy, University of Minnesota, Minneapolis, MN 55455.

L. J. Lanzerotti, Bell Laboratories, Lucent Technologies, Murray Hill, NJ 07974.

(Received March 2, 1998; revised May 14, 1998;
accepted June 3, 1998)